Augmentation of Pulmonary Reactions to Quartz Inhalation by Trace Amounts of Iron-containing Particles

Vincent Castranova,[1] Val Vallyathan,[1] Dawn M. Ramsey,[2] Jeffrey L. McLaurin,[2] Donna Pack,[1] Steven Leonard,[1] Mark W. Barger,[1] Jane Y.C. Ma,[1] Nar S. Dalal,[3] and Alex Teass[2]

[1]Health Effects Laboratory Division, National Institute for Occupational Safety and Health, Morgantown, West Virginia; [2]Division of Biomedical and Behavioral Science, National Institute for Occupational Safety and Health, Cincinnati, Ohio; [3]Department of Chemistry, Florida State University, Tallahassee, Florida

Fracturing quartz produces silica-based radicals on the fracture planes and generates hydroxyl radicals (•OH) in aqueous media. •OH production has been shown to be directly associated with quartz-induced cell damage and phagocyte activation *in vitro*. This •OH production *in vitro* is inhibited by desferrioxamine mesylate, an Fe chelator, indicating involvement of a Fenton-like reaction. Our objective was to determine if Fe contamination increased the ability of inhaled quartz to cause inflammation and lung injury. Male Fischer 344 rats were exposed 5 hr/day for 10 days to filtered air, 20 mg/m^3 freshly milled quartz (57 ppm Fe), or 20 mg/m^3 freshly milled quartz contaminated with Fe (430 ppm Fe). High Fe contamination of quartz produced approximately 57% more reactive species in water than quartz with low Fe contamination. Compared to inhalation of quartz with low Fe contamination, high Fe contamination of quartz resulted in increases in the following responses: leukocyte recruitment (537%), lavageable red blood cells (157%), macrophage production of oxygen radicals measured by electron spin resonance or chemiluminescence (32 or 90%, respectively), nitric oxide production by macrophages (71%), and lipid peroxidation of lung tissue (38%). These results suggest that inhalation of freshly fractured quartz contaminated with trace levels of Fe may be more pathogenic than inhalation of quartz alone. — *Environ Health Perspect* 105(Suppl 5):1319–1324 (1997)

Key words: Fenton reaction, silicosis, reactive oxygen species, inhalation, iron, nitric oxide, pulmonary inflammation, silica

Introduction

Occupational exposure to crystalline silica can result in the development of pulmonary fibrosis. Silicosis may develop rapidly (1–3 years) in the acute form of the disease. Acute silicosis is characterized by dyspnea, fatigue, cough, weight loss, alveolar lipoproteinosis, and diffuse fibrosis (*1*). In contrast, chronic silicosis develops over a period of 20 to 40 years. It is characterized by nodular lesions containing collagen in a spiral arrangement and may progress to massive fibrosis in which restrictive lung impairment is evident (*2,3*).

Cellular injury and tissue damage are believed to be important steps in the development of silicosis (*4*). This damage may result directly from the cytotoxicity of quartz or indirectly from oxidant species produced by silica-activated pulmonary phagocytes (*5*). Such oxidants may include superoxide anion (O_2^-), hydrogen peroxide (H_2O_2), hydroxyl radical (•OH), nitric oxide (NO•), and peroxynitrite (*6,7*).

Acute silicosis is associated with the generation of freshly fractured quartz dust in occupations such as sandblasting, rock drilling, tunneling, and silica milling. When crystalline quartz is fractured, silicon (•Si) and silicon oxyl radicals (Si-•O) respectively are formed on the fracture planes (*8*). On contact with aqueous media, these surface radicals generate •OH (*9*). The Fe chelator desferrioxamine significantly reduces this •OH production by freshly fractured quartz in water (*10*). This suggests that trace contamination of quartz with ferrous Fe can enhance •OH generation via a Fenton-like reaction as follows:

$$\text{Si–}^{\bullet}\text{O} + H_2O \rightarrow \text{SiOH} + {}^{\bullet}\text{OH}$$
$$\text{Si–}^{\bullet}\text{O} + {}^{\bullet}\text{OH} \rightarrow \text{SiOOH}$$
$$\text{SiOOH} + H_2O \rightarrow \text{SiOH} + H_2O_2$$
$$Fe^{2+} + H_2O_2 \rightarrow Fe^{3+} + {}^{\bullet}\text{OH} + OH^-$$

In vitro, freshly fractured quartz causes greater peroxidation of membrane lipids, greater membrane leakage, and a greater decrease in cell viability than aged quartz. Freshly fractured quartz is also a more potent stimulant of reactive species production by alveolar macrophages (AM) *in vitro* (*9,11*). In comparison to aged quartz, inhalation of freshly milled quartz results in a significantly enhanced cytotoxicity (lipid peroxidation of lung tissue and lavage levels of red blood cells [RBC], protein, and lysosomal enzymes) and elevated inflammation (lavageable neutrophils, generation of oxidant species from AM, and histological scoring of lung infiltrates) (*12,13*). Evidence suggests that a direct relationship exists between •OH generation and cytotoxicity, as the production of both •OH- and quartz-induced biological reactions decrease in a similar fashion with time after fracturing (*9,11*).

Because Fe enhances •OH generation by freshly fractured quartz and a relationship exists between •OH production and the cytotoxic potency of quartz, the question was whether trace amounts of Fe would increase the pulmonary responses to inhaled quartz. To resolve this question, we conducted an inhalation exposure in which rats were exposed to filtered air, freshly milled quartz with low Fe contamination, and freshly milled quartz containing 7.5 times more Fe contamination. Low and high Fe contamination of quartz was achieved by altering the length of the polyethylene delivery tube of the stainless steel screw feeder. The following pulmonary responses to quartz inhalation (20 mg/m^3, 5 hr/day, 10 days) were monitored 1 day

This paper is based on a presentation at The Sixth International Meeting on the Toxicology of Natural and Man-Made Fibrous and Non-Fibrous Particles held 15–18 September 1996 in Lake Placid, New York. Manuscript received at *EHP* 26 March 1997; accepted 23 April 1997.

Address correspondence to Dr. V. Castranova, PPRB/HELD/NIOSH, 1095 Willowdale Road (M/S 2015), Morgantown, WV 26505. Telephone: (304) 285-6056. Fax: (304) 285-5938. E-mail: vic1@cdc.gov

Abbreviations used: AM, alveolar macrophage(s); CL, chemiluminescence; ESR, electron spin resonance; •OH, hydroxyl radical(s); O_2^-, superoxide anion; PBN, *N-tert*-butyl-phenylnitrone; PHPA, 4-hydroxyphenylacetic acid; RBC, red blood cell(s); •Si, silicon radical; Si-O•, silicon oxyl radical.

postexposure: lavageable RBC, AM, and leukocytes; production of reactive species from AM; and lipid peroxidation of lung tissue.

Methods

Experimental Design

Male Fischer 344 rats (7 weeks of age) were divided into three groups of 20 rats each (filtered air controls, freshly milled quartz with low Fe contamination, and freshly milled quartz with high Fe contamination) and housed in two 10 m^3 Hinners-type walk-in chambers (quartz exposed) or a 5 m^3 Hinners-type chamber (air control). Freshly milled quartz was generated in an air jet mill (Trost Gem-T Research Model Type 1047 [Garlock Inc., Newtown, Pa] fitted with a polyurethane liner; P-jet pressure of 70 psi and an O-jet pressure of 100 psi). Low and high Fe contamination of quartz, i.e., quartz with low Fe contamination and quartz with high Fe contamination were achieved by adjusting the length of the screw feeder delivery tube (6.35 vs 15 cm to produce low vs high Fe contamination, respectively). Rats were exposed 5 hr/day for 10 days and were sacrificed 1 day postexposure for determination of biological responses. Details of the quartz dose, particle diameter, and trace metal contamination for the exposure groups are given in Table 1. Note that both quartz inhalation groups were exposed to particles of the same size (2.0–2.1 µm) and at the same dose (21–19 mg/m^3). The major difference between the two quartz aerosols was their trace metal content (57 ppm Fe for low Fe contamination and 430 ppm for high Fe contamination).

Generation of Freshly Milled Silica

Freshly fractured α-quartz was prepared from a stock IOTA lot 11383 quartz sample obtained from Unimin Corporation (Spruce Pine, NC). This stock quartz had a mass mean diameter of 191 µm and was semiconductor grade in purity, i.e., greater than 99% pure crystalline silica (SiO_2) as determined by X-ray diffraction analysis under scanning electron microscopy and optical microscopic examination under polarized light. Freshly fractured α-quartz was prepared as follows: stock of quartz dust was supplied by an AccuRate Series 100 dry material feeder (AccuRate, Whitewater, WI) with a 6.4-mm diameter stainless steel helix and a polyethylene delivery tube to a Trost Gem-T Research Model Type 1047 jet mill (Garlock, Newtown, PA) fitted with a polyurethane liner and stainless steel jets and operated with dry, charcoal-scrubbed compressed air at a P-jet pressure of 480 kPa (70 psi) and an O-jet pressure of 690 kPa (100 psi). The difference in trace metal content of the two quartz aerosols is due to stainless steel contamination from the dry material feeder. The longer the stock quartz remained in contact with the stainless steel helix, the higher the resulting contamination. Shortening the length of the polyethylene delivery tube shortened the contact time, thus lowering the stainless steel content of dust going to the jet mill.

Inhalation Exposure

The air supply to the animal chambers was rough filtered; chilled or heated to 16°C; reheated to 23°C (feedback control from the chambers); passed through a high efficiency particle filter, a charcoal bed, and a medium efficiency filter; and rehumidified with a steam humidifier. Air flow through the animal chambers was 12 air changes/hr and pressure in the chambers was held to 0.25 cm of water less than in the laboratory. The aerosol of freshly milled α-quartz was passed directly from the air jet mill via 16 and 19 mm (inside diameter) tubing through a BGI Aero-2 cyclone (BGI Inc., Waltham, MA) to the mixing chamber in the air duct 46 cm upstream of the exposure chamber. To aid mixing of the two streams, the juncture was 3 cm downstream of an orifice plate and 20 cm upstream of a circular baffle centered in the duct. The static charge on the dust was neutralized by a Static Control Services Model PFC-20 pulse flow controller (Static Control Service, Palm Springs, CA) with a Model AN-6 ionizing air nozzle located about 5 cm upstream of the mixing chamber. Exposures were conducted during the animals' dark cycles (i.e., during their active periods). Preliminary experiments with a fog generator revealed that baffling resulted in single-pass flow of air through the animal cages within the exposure chambers.

Temperature (18.5–24.2°C), humidity (37–68%), and ammonia levels in the chambers were monitored continuously. Filter samples of the chamber atmospheres were obtained continuously to determine dust concentration by gravimetric analysis. Additional filter samples were obtained to monitor trace contaminants, dust activity (i.e., H_2O_2production), surface radicals by electron spin resonance (ESR) spectroscopy, and particle size by scanning electron microscopy. The mass median aerodynamic diameter of the quartz particles was determined using a nine-stage Andersen cascade impactor ACFM particle-sizing sampler (Andersen Samplers, Atlanta, GA).

Measurement of Surface Radicals

Surface reactivity of freshly milled and aged quartz was determined by monitoring surface free radicals using ESR spectroscopy. ESR spectra were obtained with a Bruker Model ER300 spectrometer (Braker Instrument Corp., Billerica, MD) interfaced with an ASPECT 3000 microcomputer (Braker Instrument Corp.). The filter samples of dust were rolled, placed into a quartz ESR sample tube, and inserted into the center of the ESR cavity. All measurements were conducted at room temperature. The following settings were used: microwave power = 13 dB, microwave frequency = 9.53 GHz, modulation frequency = 100 kHz, modulation amplitude = 1 G, and receiver phase = 0 or 180. Silicon-based radical sites were characterized by ESR spectra centered around $g = 2.0015$. Surface activity was determined from peak height and expressed as signal height per milligram of quartz.

Table 1. Characteristics of exposure aerosols.

Group	SI dose,[a] mg/m^3	Particle diameter,[b] µm	Iron,[c] ppm
Air control	0	—	—
Si, low Fe contamination	21 ± 0.1	2.0 (1.9)	57 ± 33
Si, high Fe contamination	19 ± 0.1	2.1 (2.0)	430 ± 73

[a]Silica concentration within the exposure chambers was determined gravimetrically from filter samples. Mean ± SD (n=54). [b]Mass median aerodynamic diameter was determined using a nine-stage Andersen cascade impactor ACFM particle-sizing sampler (Andersen Samplers, Atlanta, GA). Median value (geometric SD) (n=3). [c]Trace Fe contamination was determined by proton-induced X-ray emission spectroscopy performed by Element Analysis Corporation (Lexington, KY). Mean ± SD (n=10). Other trace contaminants were Si with low Fe contamination:16 ppm chromium, 0.6 ppm copper, 1.2 ppm manganese, 7.2 ppm nickel, 1.3 ppm zinc, and 11 mg/g carbon. Carbon was measured by Galbraith Laboratories (Knoxville, TN) (n=5). Si with high Fe contamination:107 ppm chromium, 2.0 ppm copper, 11 ppm manganese, 47 ppm nickel, 0.7 ppm zinc, and 7.9 mg/g carbon.

Measurement of Silica Reactive Products

Generation of reactive products by freshly fractured quartz in aqueous media was determined by monitoring H_2O_2 production fluorometrically. The peroxidase-catalyzed oxidation of 4-hydroxyphenylacetic acid (PHPA) by H_2O_2 yields a strongly fluorescent dimer of PHPA (*14*). In our application, the quartz-laden filter was placed into 10 ml of buffer solution (5 mM $KNaHPO_4$; pH 7) and sonicated for 1 min. The filter was then rinsed with deionized water to remove residual dust. The suspension was agitated at 25°C for 30 min to allow efficient transfer of H_2O_2 into the solution. The supernatant was made 0.024 mM in PHPA and 8.9 activity U/ml in peroxidase and stored in the dark for 30 min to allow for reaction. The pH was then adjusted to greater than 10 and analysis was carried out with a flow injection system and a fluorescence detector (excitation 320 nm, emission 420 nm). The system was calibrated with standard solutions of H_2O_2 and measurements were corrected for sample blank and volume dilution.

Determination of Lavageable Cells

Animals were anesthetized and lungs were lavaged 10 times with 8-ml aliquots of Ca^{2+}, Mg^{2+}-free phosphate-buffered medium (145 mM NaCl, 5 mM KCl, 1.9 mM NaH_2PO_4, 9.35 mM Na_2HPO_4, and 5.5 mM glucose; pH 7.4). Lavage fluid was centrifuged, and cells were collected, washed, and resuspended in HEPES-buffered medium (145 mM NaCl, 5 mM KCl, 10 mM HEPES, 5.5 mM glucose, and 1 mM $CaCl_2$; pH 7.4). Cell counts were obtained using an electronic cell counter. Cell differentials were determined using a cell sizing attachment and characteristic cell volumes to count RBC, leukocytes (lymphocytes and granulocytes), and AM (*15*).

Measurement of Alveolar Macrophage Activity

Chemiluminescence (CL) generated from pulmonary phagocytes was measured at 37°C in the presence of 8 µg% luminol using a Berthold LB953 luminometer (Wallac, Gaithersburg, MD). AM (7.5×10^5 cells) were suspended in 0.75 ml of HEPES-buffered medium and preincubated at 37°C for 10 min prior to being placed into the luminometer. Zymosan-stimulated CL (counts per minute with zymosan minus counts per minute at rest) was measured in the presence of 2 mg/ml unopsonized zymosan added just before measuring CL. Note that granulocytes do not respond to unopsonized zymosan (*15*). NO synthase-dependent CL (counts per minute with zymosan minus counts per minute with zymosan plus L-NAME [N*w*-nitro-L-arginine methyl ester]) was determined as the amount of zymosan-stimulated CL that was inhibitable by 1 mM L-NAME added during the preincubation period.

Oxygen radical generation from alveolar phagocytes was measured with an electron spin resonance spectrometer using a radical spin trap. AM (5×10^5 cells/ml) obtained from the three groups of animals were incubated with 0.1 M *N-tert*-butyl-phenylnitrone (PBN) for 1 hr at 37°C in an oscillating water bath. Control experiments were carried out without cells and without PBN. The reaction was terminated by the addition of 5 ml chloroform:methanol (2:1) and total lipids were extracted. The chloroform was evaporated in a boiling water bath and the lipid was reconstituted in 0.5 ml chloroform and transferred to nuclear magnetic resonance quartz tubes. On the basis of a method of Vallyathan and colleagues (*16*), ESR measurements of the chloroform extracts were made within 1 hr using a Varian E-109 ESR spectrophotometer (Varian Associates, Palo Alto, CA) operating at X-band (9.7 GHz) at the following spectrometer settings: receiver gain, 3.2×10^5; microwave power, 50 mW; modulation amplitude, 2 G; scan time, 100 sec; time constant, 1 sec; magnetic field, 3417 ± 50 G. ESR spectra were recorded and integrated for three scans as a measure of reactive oxygen species generated from phagocytes. Scaling and analysis of the spectra were made using the EPR (U.S. EPR, Clarksville, MD) DAP 2.0 program.

Measurement of the Lung Lipid Peroxidation

Lipid peroxidation of lung tissue from the three groups of animals was monitored by measuring thiobarbituric acid reactive substances generated during incubation of lung slices for 1 hr in a buffered medium without any other stimulation, according to the method of Hunter and co-workers (*17*). Thin lung tissue slices (300–450 mg) were incubated in phosphate-buffered medium at pH 7.4 for 1 hr at 37°C in a shaking water bath. The reaction was terminated by the addition of 0.3 ml 5 N HCl and 0.625 ml 40% trichloroacetic acid. After mixing, 0.625 ml thiobarbituric acid was added to the reaction mixture, mixed, and heated in a water bath at 95°C for 20 min. The thiobarbituric acid-reactive substances developed a color that was measured after cooling at 540 nm and compared with malondialdehyde reaction with thiobarbituric acid. Malondialdehyde production was calculated from a standard graph that was made using the same reagents and known concentrations of malondialdehyde. Control experiments were carried out without lung tissues, with inactivated lung tissue, and in the presence of an antioxidant (butyl hydroxy toluene) to inhibit lipid peroxidation.

Statistical Analysis

Data are means ± standard errors of 4 to 8 values determined from separate rats. Data were analyzed by analysis of variance to determine significance at $p < 0.05$.

Results

Freshly fracturing quartz in a jet mill breaks Si-O bonds and generates $^{\bullet}$Si and Si-O$^{\bullet}$ radicals on the fracture planes. As shown in Figure 1, trace contamination with stainless steel particles has no effect on the generation of these surface radicals. Indeed, there is no difference in the intensity of the ESR signal produced by quartz with low Fe contamination compared with that produced by quartz with high Fe contamination after jet milling (intensity ratio of 1 and 0.93 for Si [low Fe contamination] and Si [high Fe contamination], respectively).

In contrast, once placed in aqueous media, quartz with high Fe contamination produces more reactive species than quartz

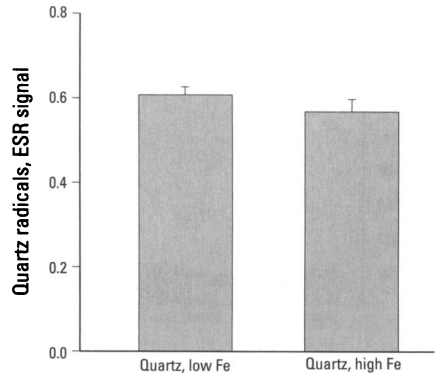

Figure 1. $^{\bullet}$Si and Si-O$^{\bullet}$ radicals on the fracture planes of quartz after milling. Surface radicals were measured by ESR. Quartz with low Fe contamination and quartz with high Fe contamination contain 57 and 430 ppm Fe particles, respectively. Data represent signal heights (means ± SEM from four chamber samples).

with low Fe contamination (Figure 2). These data suggest that trace contamination of quartz with Fe particles (430 ppm) is sufficient to allow Fenton-like reactions to occur and result in enhanced generation of reactive species by freshly fractured quartz.

Bronchoalveolar lavage indicates that inhalation of quartz with high Fe contamination causes significantly more damage to the alveolar air–blood barrier than an equal exposure to quartz with low Fe contamination, as measured by the lavage yield of RBC (Figure 3). Freshly milled silica contaminated with high Fe is also more inflammatory than milled silica with low Fe contamination, as judged by the infiltration of leukocytes (lymphocytes and granulocytes) into the airspaces of the lung (Figure 3).

The activity of AM harvested from quartz-exposed rats was determined by monitoring: zymosan-induced chemiluminescence, NO-dependent chemiluminescence, and the production of oxygen radicals using ESR and a spintrap. Inhalation of quartz contaminated with stainless steel Fe particles, i.e., quartz with high Fe contamination, significantly increases zymosan-stimulated chemiluminescence from AM above that seen after exposure to quartz with low Fe contamination (Figure 4). Similar Fe enhancement is observed when NO-dependent (L-NAME-inhibitable) macrophage chemiluminescence is monitored in response to zymosan (Figure 5) and when measuring the generation of oxygen radicals by alveolar phagocytes (Figure 6).

The enhanced production of reactive species in response to inhalation of quartz with high Fe contamination compared to quartz with low Fe contamination results in a greater level of lipid peroxidation in lung tissue exposed to high Fe-contaminated quartz (Figure 7). This increased lung damage may explain the breakdown of the alveolar air–blood barrier suggested in Figure 3, i.e, the increase in lavageable RBC.

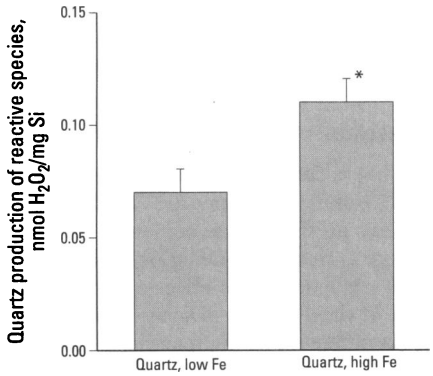

Figure 2. Production of reactive species by freshly fractured quartz in aqueous medium. Quartz with low Fe contamination and quartz with high Fe contamination contain 57 and 430 ppm Fe particles, respectively. Data represent means ± SEM from eight chamber samples. *Significant increase above quartz with low Fe contamination ($p<0.05$).

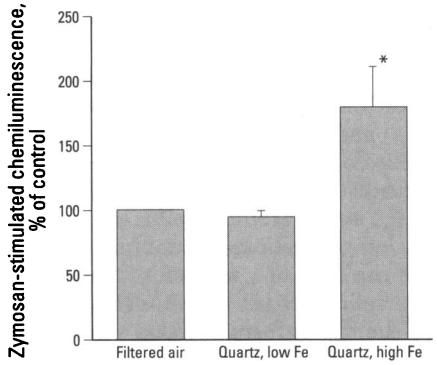

Figure 4. Zymosan-stimulated chemiluminescence from rat alveolar macrophages harvested by bronchoalveolar lavage 1 day after quartz exposure (20 mg/m^3, 5 hr/day for 10 days). Quartz with low Fe contamination and quartz with high Fe contamination contain 57 and 430 ppm Fe particles, respectively. Data are means ± SEM from four rats. *Significant increase above quartz with low Fe contamination ($p<0.05$).

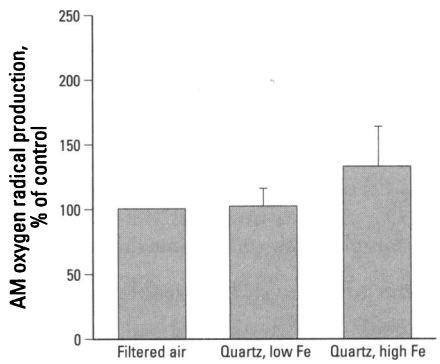

Figure 6. Generation of oxygen radicals produced by rat alveolar phagocytes harvested by bronchoalveolar lavage 1 day after quartz exposure (20 mg/m^3, 5 hr/day for 10 days). Oxygen radicals are measured by ESR using a spin trap. Quartz with low Fe contamination and quartz with high Fe contamination contain 57 and 430 ppm Fe particles, respectively. Data are means ± SEM from four rats.

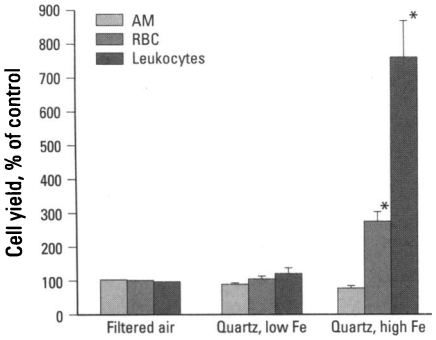

Figure 3. AM, RBC, and leukocytes (lymphocytes and granulocytes) harvested by bronchoalveolar lavage 1 day after quartz exposure (20 mg/m^3 , 5 hr/day for 10 days). Quartz with low Fe contamination and quartz with high Fe contamination contain 57 and 430 ppm Fe particles, respectively. Data are means ± SEM from eight rats. *Significant increase above quartz with low Fe contamination ($p<0.05$).

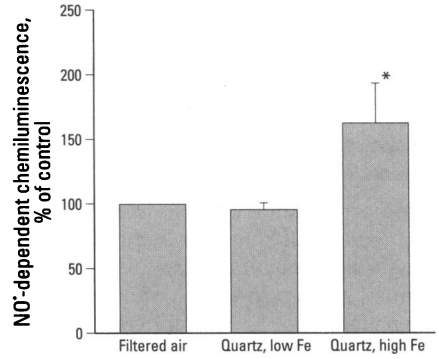

Figure 5. NO-dependent chemiluminescence from rat AM harvested by bronchoalveolar lavage 1 day after quartz exposure (20 mg/m^3, 5 hr/day for 10 days). Quartz with low Fe contamination and quartz with high Fe contamination contain 57 and 430 ppm Fe particles, respectively. Data are means ± SEM from four rats. *Significant increase above quartz with low Fe contamination ($p<0.05$).

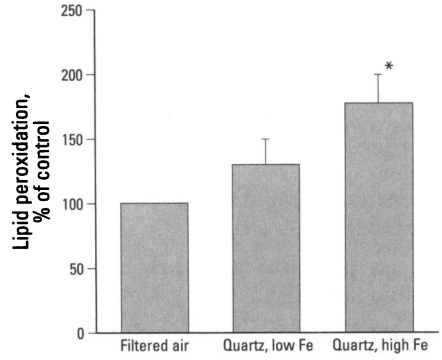

Figure 7. Lipid peroxidation of lung tissue measured as malondialehyde production 1 day after quartz exposure (20 mg/m^3, 5 hr/day for 10 days). Quartz with low Fe contamination and quartz with high Fe contamination contain 57 and 430 ppm Fe particles, respectively. Data are means ± SEM from four rat lungs. *Significant increase above quartz with low Fe contamination) ($p<0.05$).

Discussion

The results of this investigation indicate that pulmonary responses 1 day after inhalation exposure to α-quartz are rather small when the quartz used is of semiconductor purity and efforts are employed to minimize trace metal contamination by the dust generation system. The simple increase in the length of the delivery tube of the screw feeder is sufficient to increase the Fe contamination of silica from 57 to 430 ppm. Such trace Fe contamination increases the generation of reactive species by silica in aqueous media by 52%. Trace Fe contamination also results in augmentation of pulmonary responses to quartz inhalation (Table 2). That is, in comparison to quartz with low Fe contamination, quartz with high Fe contamination increases leukocyte recruitment by 537%, lavagable RBC by 157%, phagocyte production of oxygen radicals by 32%, AM zymosan-stimulated chemiluminescence by 90%, NO-dependent chemiluminescence from AM by 71%, and lung lipid peroxidation by 38%.

Ghio et al. (*18*) have proposed that silica-induced lung disease is mediated by surface coordination with Fe and the subsequent generation of ˙OH via the Fenton reaction. Indeed, silica–Fe complexation has been demonstrated in rat lungs after intratracheal instillation of silica (*19*). *In vitro* treatment of silica with desferrioxamine mesylate (an Fe chelator) decreases silica-induced oxidation of lung surfactant and the silica-stimulated respiratory burst of AM (*20,21*). Similarly, desferrioxamine decreases the ability of freshly fractured quartz to generate ˙OH in aqueous media (*10*). Such pulmonary production of ˙OH has been demonstrated in quartz-exposed rats and has been associated with lung inflammation (*22*). The results of the current investigation support the hypothesis that trace Fe contamination can augment the generation of oxidants by quartz and enhance its inflammatory and cytotoxic potency in the lung. In addition, our results extend the hypothesis by demonstrating that this augmentation is possible with particulate Fe contamination as might be experienced in occupational settings such as rock drilling or sandblasting.

Table 2. Increased activity of quartz with high Fe contamination.

Parameter	Percent increase quartz, high Fe: quartz, low Fe
Quartz reactive species	52
Lavage RBC	157
Lavage leukocytes	537
AM zymo-stim CL	90
AM NO˙-dependent CL	71
AM oxygen radicals	32
Lung lipid peroxidation	38

Zymo-stim, zymosan-stimulated.

In contrast to the above hypothesis that Fe contamination increases the cytoxicity of quartz, Nolan et al. (*23*) have reported that Fe chloride solutions decrease the *in vitro* hemolytic potential of quartz by neutralizing the negative surface charge of quartz. Similarly, Fe chloride solutions can decrease quartz-induced hydrogen peroxide secretion from AM *in vitro* (*24*). Particulate Fe is also protective against quartz-induced pulmonary inflammation (neutrophil recruitment) after intratracheal instillation of carbonyl Fe plus quartz (*24*). This apparent conflict is resolved by an analysis of the Fe dose required to neutralize the negative surface charge of quartz and result in significant detoxification. In solution, as much as 1 M Fe chloride is required to eliminate the negative surface charge of quartz, whereas as a particulate, Fe must be 12-fold in excess of quartz for depression of toxicity to become apparent (*24*). In contrast, quartz–Fe complexes in the lung are associated with only trace levels of Fe (*19*). Furthermore, the current investigation clearly demonstrates that trace contamination of quartz with Fe particles (430 ppm) enhances pulmonary inflammation and lung damage.

In this study, the reactivity of the freshly fractured quartz was associated with the level of Fe contamination. However, it must be noted that the two quartz aerosols investigated in this study really differed in their contamination by stainless steel particles. Thus, as demonstrated in Table 1, amounts of numerous trace metals (chromium, copper, manganese and nickel) as well as Fe were elevated in the more toxic quartz sample. Emphasis has been placed on Fe because of the extensive literature associating Fe with the generation of ˙OH via the Fenton reaction. However, evidence exists that chromium (Cr^{3+}) can also generate ˙OH in the presence of H_2O_2(*25*). In addition, nickel (Ni^{2+}) has been reported to generate ˙OH from hydroperoxides but only in the presence of oligopeptides such as glutathione (*26*).

In conclusion, the negative surface charge of crystalline quartz contributes to its unique toxicity. Gross quantities of Fe can coat the quartz surface and neutralize this surface charge to partially detoxify quartz. However, the required Fe:quartz particulate ratio of greater than 12:1 is not likely in occupational settings where silicosis is a concern. In contrast, trace contamination of quartz with Fe may occur in rock drilling or sand blasting. Such trace Fe could catalyze the generation of ˙OH by freshly fractured quartz leading to increased lung damage and inflammation, as shown in this investigation.

REFERENCES

1. Banks DE. Acute silicosis. In: Occupational Respiratory Diseases (Merchant JA, Boehlecke BA, Taylor G, Pickett-Harner M, eds). Washington:National Institute for Occupational Safety and Health, 1986;239–241.
2. Parkes WR. Occupational Lung Disorders. 2nd ed. Boston:Butterworths, 1982.
3. Ziskind M, Jones RN, Weill H. Silicosis. Am Rev Respir Dis 113:643–665 (1976).
4. Davis GS. The pathogenesis of silicosis. Chest 89:161–169 (1986).
5. Lapp NL, Castranova V. How silicosis and coal workers' pneumoconiosis develop—a cellular assessment. Occup Med State of the Art Rev 8:35–56 (1993).
6. Weiss SJ, Lo Buglio AF. Biology of disease: phagocyte-generated oxygen metabolites and cellular injury. Lab Invest 47:5–18 (1982).
7. Castranova V, Antonini JM, Reasor MJ, Wu L, VanDyke K. Oxidant release from pulmonary phagocytes. In: Silica and Silica-Induced Lung Disease (Castranova V, Vallyathan, Wallace WE, eds). Boca Raton, FL:CRC Press, 1996;185–196.
8. Bolis V, Fubini B, Venturello G. Surface characterization of various silica. J Thermal Anal 28:249–257 (1983).
9. Vallyathan V, Shi X, Dalal NS, Irr W, Castranova V. Generation of free radicals from freshly fractured silica dust: potential role in acute silica-induced lung injury. Am Rev Respir Dis 138:1213–1219 (1988).

10. Dalal NS, Shi X, Vallyathan V. Potential role of silicon-oxygen radicals in acute lung injury. In: Effects of Mineral Dusts on Cells (Mossman BT, Bégin RO, eds). NATO ASI Series, Vol H30. Berlin:Springer-Verlag, 1989;265–272.
11. Castranova V, Dalal NS, Vallyathan V. Role of surface free radicals in the pathogenicity of silicosis. In: Silica and Silica-Induced Lung Diseases (Castranova V, Vallyathan V, Wallace WE, eds). Boca Raton, FL:CRC Press, 1996; 91–106.
12. Castranova V, Pailes WH, Dalal NS, Miles PR, Bowman L, Vallyathan V, Pack D, Weber KC, Hubbs A, Schwegler-Berry D et al. Enhanced pulmonary response to the inhalation of freshly fractured silica as compared with aged dust exposure. Appl Occup Environ Hyg 11:937–941 (1996).
13. Vallyathan V, Castranova V, Pack D, Leonard S, Shumaker J, Hubbs AF, Shoemaker DA, Ramsey DM, Pretty JR, McLaurin JL et al. Freshly fractured quartz inhalation leads to enhanced lung injury and inflammation: potential role of free radicals. Am J Respir Crit Care Med 152:1003–1009 (1995).
14. Guilbault GG, Brignac PJ Jr, Juneau M. New substrates for the fluorometric determination of oxidative enzymes. Anal Chem 40:1256–1263 (1968).
15. Castranova V, Jones T, Barger MW, Afshari A, Frazer DG. Pulmonary responses of guinea pigs to consecutive exposure to cotton dust. In: Proceedings of the 14th Cotton Dust Research Conference, 12–13 June 1990, Las Vegas, NV (Jacobs RR, Wakelyn PJ, Domelsmith LN, eds). Memphis, TN:National Cotton Council, 1990;131–135.
16. Vallyathan V, Mega JF, Shi X, Dalal NS. Enhanced generation of free radicals from phagocytes induced by mineral dusts. Am J Respir Cell Mol Biol 6:404–413 (1992).
17. Hunter FE Jr, Gebicki JM, Hoffsten PE, Weinstein J, Scott A. Swelling and lysis of rat liver mitochondria induced by ferrous ions. J Biol Chem 238:828–832 (1963).
18. Ghio AJ, Kennedy TP, Schapira RM, Crumbliss AL, Holdal JR. Hypothesis: Is lung disease after silicate inhalation caused by oxidant generation? Lancet 336:967–969 (1990).
19. Ghio AJ, Jaskot RH, Hatch GE. Lung injury after silica instillation is associated with an accumulation of iron in rats. Am J Physiol 267:L686–L692 (1994).
20. Ghio AJ, Hatch GE. Lavage phospholipid concentration after silica instillation in the rat is associated with complexed [Fe^{3+}] on the dust surface. Am J Respir Cell Mol Biol 8:403–407 (1993).
21. Ghio AJ, Kennedy TP, Whorton AR, Crumbliss AL, Hatch GE, Holdal JR. Role of surface complexed iron in oxidant generation and lung inflammation induced by silicates. Am J Physiol 263:L511–518 (1992).
22. Schapira RM, Ghio AJ, Effros RM, Morrisey J, Almagro UA, Dawson CA, Hacker AD. Hydroxyl radical production and lung injury in the rat following silica or titanium dioxide instillation *in vivo*. Am J Respir Cell Mol Biol 12:220–226 (1995).
23. Nolan RP, Langer AM, Harrington JS, Oster G, Selikoff H. Quartz hemolysis as related to its surface functionalities. Environ Res 26:503–520 (1981).
24. Cullen RT, Hagen S, Donaldson K, Vallyathan V. Protection by iron against the toxic effects of quartz. Inhaled Particles, 25–30 September 1996, Cambridge. Ann Occup Hyg (in press).
25. Shi X, Dala NS, Kasprzak KS. Generation of free radicals from hydrogen peroxide and lipid hydroperoxides in the presence of Cr (III). Arch Biochem Biophys 302:294–299 (1993).
26. Shi X, Dala NS, Kasprzak KS. Generation of free radicals from lipid hydroperoxides by Ni^{2+} in the presence of oligopeptides. Arch Biochem Biophys 299:154–162 (1992).